Rotating Molecules Trapped in Pseudorotating Cages

J. Manz

Contribution from the Lehrstuhl für Theoretische Chemie, Technische Universität München, D-8046 Garching, Germany. *Received August 30, 1979*

Abstract: A model of the rotating molecule in the pseudorotating cage is developed. The pseudorotation arises from host molecular relaxations into the minimum-energy configuration, depending on the guest molecular orientation. The cage's shape and alignment thus resemble those of the molecule, provided that lattice relaxations are faster than the rotation. The pseudorotation yields two effects which are incorporated in the generalized Devonshire model of matrix-isolated rotating molecules: the moment of inertia increases, and the cell potential of the undistorted lattice is replaced by that of the relaxed lattice. As an example, the librational spectrum of CO molecules imbedded in argon is considered.

I. Introduction

Rotating or librating molecules in solid matrices may induce an interesting effect which we wish to present in this paper. The effect is illustrated in Figure 1, and a qualitative description is as follows.

For a given molecular orientation, the neighboring host molecules relax into new equilibrium positions.[1-5] Therefore, the host molecules form a cage which differs from the undistorted lattice cage. Typically, the shape of the distorted cage resembles that of the guest molecule; e.g., an ellipsoidal molecule may destroy the cubic host lattice symmetry and induce ellipsoidal deformations in its vicinity.[5,6] When the guest molecule is slowly reoriented, the cage deformations may follow the molecule owing to the nonrigidity of the host lattice. Thus, in the previous example, an ellipsoidal molecule may always find itself surrounded by an ellipsoidal cage orientated along the momentary molecular orientation. The guest molecule then rotates in a synchronously rotating cage. Since the cage rotation is established by cooperative small deviations of host molecular equilibrium positions from undistorted lattice sites (and not by actually rotating host molecules) we call it a *pseudorotation*.

An important consequence of the synchronous molecular rotation and cage pseudorotation is the effective increase of the molecular moment of inertia. We shall show below in section II that it may exceed the moment of inertia of the molecule in the gas phase by 50% or even more.

The larger effective moment of inertia in turn may lead to interesting observable consequences. Firstly, it influences the rotational or librational spectra of matrix isolated molecules. An example will be presented below in section III. Secondly, together with the lattice relaxations it may affect the rates of vibrational energy relaxation and transfer via the role of the molecular rotational motion which has been determined in recent experiments[7-14] and theories.[3,14-25]

The coupled molecular and host rotation and pseudorotation should, of course, be described rigorously using quantum mechanics, and including all the couplings of the molecular vibrational, librational, and translational degrees of freedom with the lattice phonon modes. The corresponding theoretical framework has been developed in the past,[26-31] culminating presently in such different approaches as those of Berkowitz and Gerber,[20] of Zumofen, Dressler, and Kunsch[3,23-25] (see also ref 32), and of Friedmann and Kimel.[53] However, here we shall restrict ourselves to developing a simple semiclassical model. We hope that the model may serve as a guide to the more sophisticated quantum-mechanical approach. Essentially, the model describes the rotation of the guest molecule with its larger effective moment of inertia in the potential field induced by the host molecules of the pseudorotating cage. With a quantum-mechanical treatment of this rotational motion, the present model then is an extension of the classic approaches by Pauling[33] and Devonshire[34] (see also ref 6 and 35–37).

To verify the predictions in a first example, we shall explicitly consider the case of a CO molecule imbedded in an argon matrix. This system has been intensively studied in the past, both experimentally[14,38-43] and theoretically.[5,15,22,26,30,44-49] In particular, Dubost observed a weak spectroscopic band which he assigned to isolated librating CO molecules.[39,40,43] From a careful consideration of previous theoretical approaches he concluded that none of them could satisfactorily account for the properties of the librational band[39,40] (see, however, ref 43 for a very recent discussion of the width of the band). In this paper, we propose an explanation of the experimental findings using the present model.

This paper is structured as follows. In section II we derive the increase of the molecular moment of inertia due to the pseudorotation of the cage. In section III, we consider the orientational dependence of the molecule–cage interaction potential, taking into account the pseudorotational cage deformations. Both effects, i.e., the effective moment of inertia and the effective interaction potential, are used to generalize the Devonshire cell model of matrix-isolated rotating or librating molecules. Results, discussions, and conclusions are in sections IV–VI.

II. The Effective Moment of Inertia of the Rotating Molecule in the Pseudorotating Cage

In this section, we derive the effective moment of inertia of the rotating molecule in the pseudorotating cage. For this purpose, we consider first the lattice relaxations around a single vacancy substitutional molecule.

As an example, we illustrate in Figure 2 the Ar-matrix relaxation around a CO molecule. The results are adapted from ref 5.

When the central molecule is oriented along the energetically preferential (0,0,1) crystal axis, the nearest-neighbor atoms in the polar configuration (labeled 1, 2, 3, 4, 9, 10, 11, 12 in Figure 2) are pushed away by $\approx$0.05 Å, whereas the atoms in the equatorial configuration (labeled 5, 6, 7, 8) are attracted by $\approx$0.06 Å toward the molecule (see the top panel of Figure 2). As a result, the 12 nearest-neighbor atoms form an approximately ellipsoidal cage. Its major and minor semiaxes deviate from the radius $R = 3.756$ Å of the undistorted spherical cage by only

$$\Delta R \approx 0.06 \text{ Å} \tag{1}$$

The ellipsoidal cage deformation results from the approximately ellipsoidal shape of the CO molecule.[5]

Also shown in Figure 2 is the shift of the guest molecule toward its energetically favored position. As a result, the molecular center of interaction $\vec{R}_{ci}$ coincides (by definition[26]) with

0002-7863/80/1502-1801$01.00/0

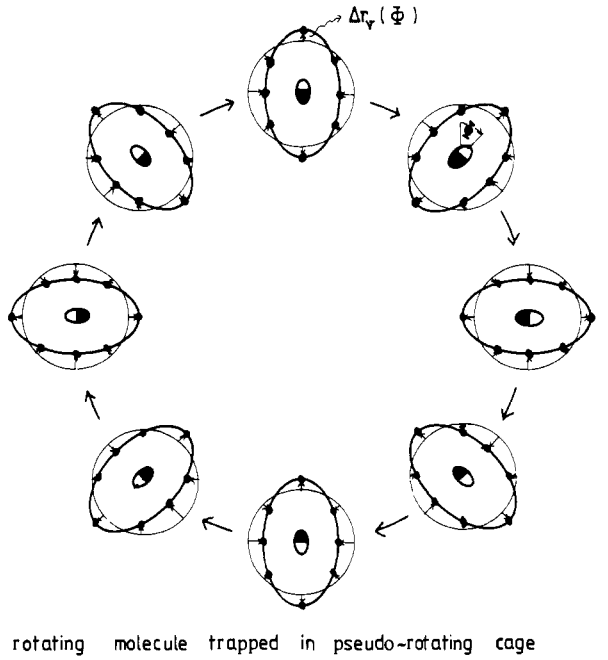

Figure 1. Rotating molecule trapped in synchronously pseudorotating cage (schematic). The molecule is shown as a black-white ellipsoid together with its nearest neighbors (black dots) in eight successive phases $\Phi = i(2\pi/8)$, $i = 0, 1, \ldots, 7$, of the full rotation. The shifts $\Delta r_\nu(\Phi)$ of the neighboring molecules from undistorted lattice sites on a sphere (thin continuous lines) toward their momentary equilibrium positions on an ellipsoid (heavy continuous lines) are indicated by little arrows. Note that a full guest molecular rotation corresponds to a double cycle of the individual shifts Δr_ν around the undistorted lattice sites.

the central lattice site, and the distance from the molecular center of mass, $\vec{R}_{cm}$, is

$$a(0,0,1) = |\vec{R}_{ci} - \vec{R}_{cm}| = 0.25 \text{ Å} \quad (2)$$

A similar pattern arises when the molecule is reoriented along the (energetically less favorable[5]) (1,1,1) direction (see the center panel of Figure 2). Again the polar atoms (now those labeled 1, 4, 5, 7, 10, 11) are pushed away (now by ≈0.07 Å), whereas the equatorial ones (labeled 2, 3, 6, 8, 9, 12) are attracted (by ≈0.06 Å) toward the central molecule. As a result, the molecule finds itself again surrounded by nearest neighbors which form an ellipsoidal cage very similar in shape to that attained in the molecular (0,0,1) direction. Furthermore, the distance of the molecular centers of interaction and mass is

$$a(1,1,1) = 0.20 \text{ Å} \quad (3)$$

i.e., also very similar to $a(0,0,1)$, eq 2.

As is indicated in Figure 2, the molecule may further move on to the (0,1,0) direction, etc. Here, by symmetry considerations, the ellipsoidal matrix cage is, of course, equivalent to the (0,0,1) cage, but now oriented along the molecular (0,1,0) direction. In summary, successive molecular reorientations with synchronous lattice deformations such as those indicated in Figure 2 provide an example of the effect shown schematically in Figure 1.

As a result, the calculations of the lattice relaxations[5] show two effects which lead to an increase of the effective molecular moment of inertia, I. One of them is well known,[26,40] i.e., the contribution due to the effective rotation of the molecular center of mass around the center of interaction

$$\Delta I_1 = Ma^2 \quad (4)$$

where M is the molecular mass, and $a = |\vec{R}_{ci} - \vec{R}_{cm}|$ is roughly independent of the molecular orientation; cf. eq 2 and 3. The

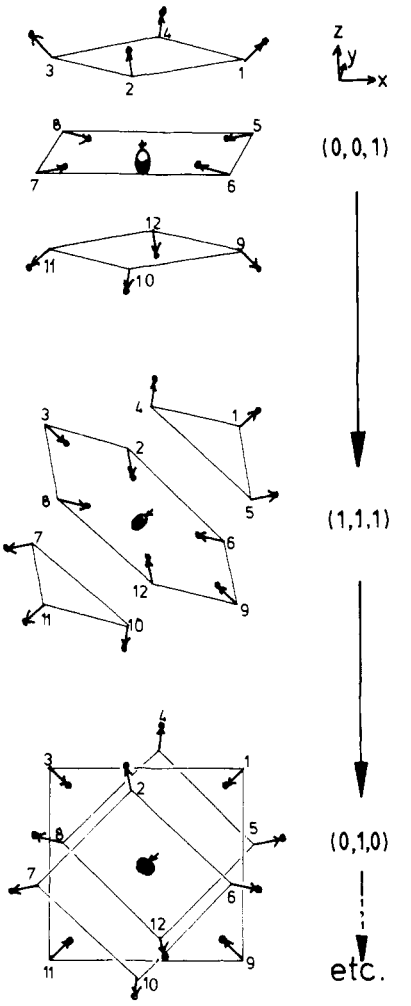

Figure 2. Rotating CO molecule in its pseudorotating Ar cage. Three successive molecular orientations along the lattice (0,0,1), (1,1,1), and (0,1,0) directions are shown in the top, center, and bottom panels, respectively. In each case, equivalent undistorted lattice sites are connected by straight lines. The little arrows indicate the host atoms' shifts toward new momentary equilibrium positions (●) (not to scale). The relaxation of the molecular center of mass away from the central site is also indicated by an arrow. As a result, the C atom is moved toward the origin.

second contribution, ΔI_2, arises from the synchronously pseudorotating cage.

In order to estimate ΔI_2, we employ the planar model illustrated in Figure 1 with the values for the cage deformations obtained above from the calculations of lattice relaxations. When the molecule is rotated by an angle Φ, the equilibrium position of neighboring atom ν oscillates around its undistorted lattice site:

$$\Delta r_\nu(\Phi) \approx \Delta r_\nu \sin(2\Phi + \delta_\nu) \quad (5)$$

The important factor 2 in eq 5 indicates that a half-rotation of the molecule suffices to induce a full cycle of the shifts $\Delta r_\nu(\Phi)$ from maximum repulsion over maximum attraction back to maximum repulsion (with amplitude Δr_ν and phase δ_ν); cf. Figure 1. The average classical kinetic energy of the pseudorotating cage then is

$$T_{rot} \approx \frac{1}{2} \sum_\nu m_\nu \overline{\Delta \dot{r}_\nu^2} \quad (6)$$

where the sum is over all nearest neighbors, and the bar indicates the time average. We shall now rewrite eq 6 in a form which indicates the corresponding effective moment of inertia. Note that, according to the model, $\Delta r_\nu(\Phi)$ depends on the molecular rotational frequency. A molecule rotating with frequency $\omega = \Phi/t$ thus induces a pseudorotation of its cage

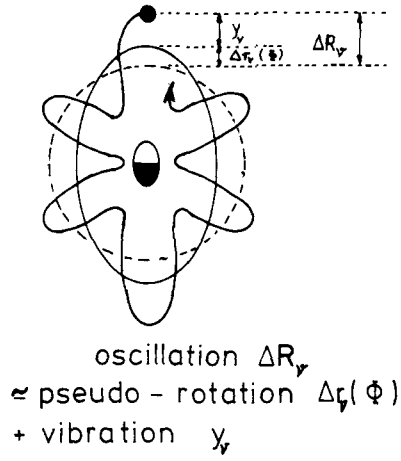

Figure 3. The motion of a neighboring host atom ν viewed from the rotating molecule. The host oscillation ΔR_ν, i.e., the deviation of the atomic position from its undistorted lattice site (illustrated by the dashed sphere), consists of the pseudorotational shift toward new momentary equilibrium positions, $\Delta r_\nu(\Phi)$ (illustrated by the heavy ellipsoid), plus the shift y_ν arising from lattice vibrations around the momentary equilibrium positions.

with kinetic energy

$$T_{\text{rot}} = \frac{1}{2}\Delta I_2 \omega^2 \tag{7}$$

where the effective moment of inertia is determined from eq 5 and 6:

$$\Delta I_2 \approx 2 \sum_\nu m_\nu \Delta r_\nu^2 \tag{8}$$

The total effective moment of inertia associated with the coupled molecular and cage rotation and pseudorotation then is

$$I = I_0 + \Delta I_1 + \Delta I_2 \tag{9a}$$

with I_0 the gas-phase molecular moment of inertia.

As an example, let us consider the case of CO in Ar. With $a \approx 0.25$ Å (cf. eq 2 and 3) in eq 4 and $\Delta r_\nu \approx 0.06$ Å (cf. eq 1) in eq 8, eq 9 reads

$$I = (8.73 + 1.75 + 3.46) \text{ amu Å}^2 \tag{9b}$$

i.e., the effective moment of inertia of CO in Ar, $I = 13.94$ amu Å^2, exceeds that of CO in gas by a factor of 1.6.

At first glance, the rather large value of ΔI_2 is quite surprising in the light of the rather small shifts $\Delta r_\nu \approx 0.06$ Å, eq 1, which enter eq 8 even squared. However, this small factor is compensated mainly by the large number of nearest neighbors, and also by the (square of) the factor 2 of eq 5, i.e., the double-speed pseudorotation in comparison with the molecular rotation.

We emphasize that eq 5–8 have been derived from a simple model and therefore serve only as approximations to the dynamically consistent quantum-mechanical description. The more realistic three-dimensional realization, Figure 2, indicates that higher order Fourier components are necessary in eq 5 for an exact description of the time dependence of the host atoms' shifts toward their momentary equilibrium positions. Furthermore, the full host atom's oscillation ΔR_ν around the undistorted lattice site consists of two parts: the "concerted" portion of the full lattice motion, i.e., the pseudorotational shift, Δr_ν, and the remaining shift y_ν which describes lattice vibrations around the *momentary* equilibrium configuration; cf. Figure 3. Clearly these motions are coupled, and the separating approximation (6) is only valid if the rotation is slower than the typical lattice vibration. Last, but not least, the sum in eq 8 should also include non-nearest-neighbor sites, but their very small amplitudes Δr_ν give only negligible contributions to ΔI_2 (see ref 5). In the following we shall neglect all these refinements which should rigorously arise from a full quantum mechanical treatment; i.e., we shall employ the approximation (9) with ΔI_1 and ΔI_2 given by eq 4 and 8, respectively.

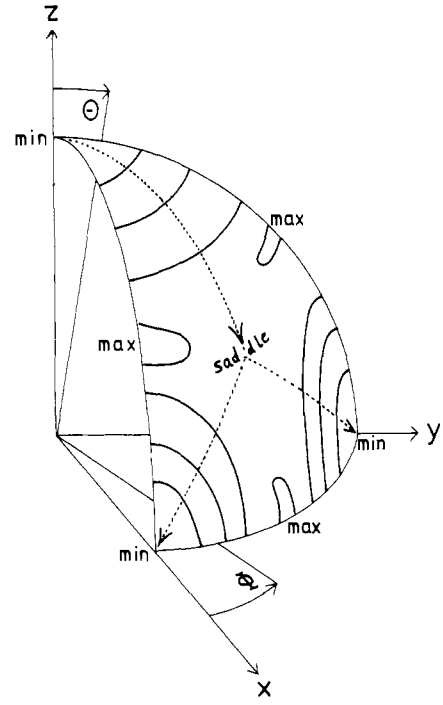

Figure 4. The orientational topology of the potential energy of CO in solid Ar. The CO center of interaction is at the origin. Heavy continuous lines indicate equipotential contours drawn on a sphere; the symbols min, saddle, and max denote the corresponding potential energy minima, saddle point, and maxima, respectively. The dashed arrows illustrate possible classical paths of molecular orientations from minima over saddle points to new minima. The branch leading from the z axis over the saddle to the y axis corresponds to the reorientation from the (0,0,1) over the (1,1,1) to the (0,1,0) directions illustrated in Figure 2.

III. The Effective Potential of the Rotating Molecule in the Pseudorotating Cage

The model of the rotating molecule in the pseudorotating cage can now be used to generalize the Devonshire cell model of librating molecules trapped in solid matrices. The Devonshire model[34] essentially aims at the computation of librational spectra of matrix isolated molecules. For this purpose, molecular gas-phase moments of inertia are used, and the molecule rotates in the potential field $V(\Theta,\Phi)$ of the molecule and the undistorted lattice. The topology of $V(\Theta,\Phi)$ is illustrated schematically in Figure 4 for the case of CO in Ar. A quantitative contour plot of the potential is shown in Figure 5 (adapted from ref 5; V has been called ΔV in ref 5).

The model of the rotating molecule in the pseudorotating cage now suggests that $V(\Theta,\Phi)$ should be replaced. In fact, the guest molecule in the (Θ,Φ) orientation (and with its center of interaction at the origin) actually has its neighboring atoms relaxed into momentary equilibrium positions. The corresponding interaction potential $\tilde{V}(\Theta,\Phi)$ is different from $V(\Theta,\Phi)$, i.e., V should be replaced by $\tilde{V}$. In other words, the synchronously pseudorotating cage does not only lead to an increased effective moment of inertia, cf. section II; it also establishes self-consistently the potential energy $\tilde{V}(\Theta,\Phi)$ for the momentary molecular orientation. Note that, vice versa, the specific geometries attained by the pseudorotating cage (such as those illustrated in Figure 2) are *defined* by the condition that, for the given molecular orientation (Θ,Φ), the potential energy of the guest molecule in the matrix should be

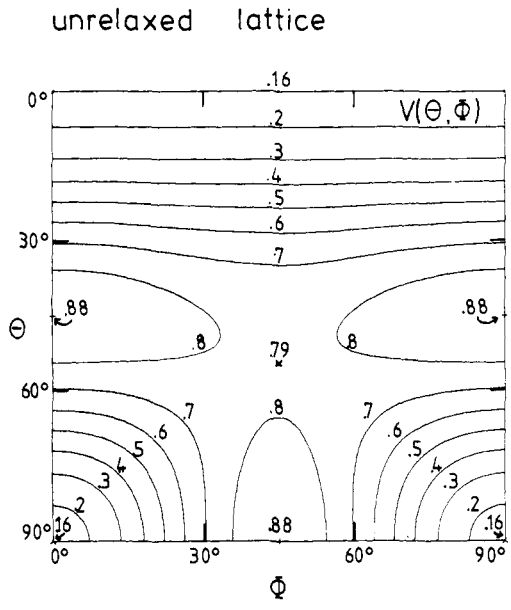

Figure 5. Potential energy surface $V(\Theta,\Phi)$ for CO in Ar, adapted from ref 5. The CO center of interaction is at the origin, whereas the host atoms are not relaxed. Numbers on the equipotential contours give the value of V in kJ mol^{-1}. ($V = 0$ corresponds to the pure Ar crystal.) A schematic spherical presentation of the potential is in Figure 4.

minimal, $\tilde{V}(\Theta,\Phi)$.[5] For example, when the molecule is oriented along the (0,0,1) or (1,1,1) directions (cf. Figure 2), the ellipsoidal lattice deformations lead to decreases from $V(0°,0°) = 0.16$ kJ mol^{-} and $V(54.7°,45°) = 0.79$ kJ mol^{-1} (cf. Figure 5) to

$$\tilde{V}(0°,0°) = -0.16 \text{ kJ mol}^{-1}$$
$$\tilde{V}(54.7°, 45°) = 0.16 \text{ kJ mol}^{-4} \quad (10)$$

respectively, in the case of CO in Ar.[5] From eq 10, the potential barrier can be estimated, $\Delta\tilde{V} \approx 0.32$ kJ mol$^{-1} \approx 27$ cm^{-1}. It is gratifying that this value is apparently in accordance with a similar barrier height deduced from the anharmonicity of the $0 \rightarrow 1$ and $1 \rightarrow 2$ librational transitions.[43]

At this point, we should like to emphasize that, in the present model, $\tilde{V}(\Theta,\Phi)$ is the minimum molecule–lattice interaction potential energy for the given molecular orientation. In particular, $\tilde{V}(\Theta,\Phi) - \tilde{V}(\Theta,\Phi)$ is not necessarily a constant; cf. eq 10. In principle it is even possible that the topologies of V and $\tilde{V}$ differ, although the approximately constant shape of the pseudorotating cage suggests rather smooth variations in $V - \tilde{V}$. In any case, the present model goes beyond that of Lee,[6] which assumes that the matrix cage retains its global minimum energy configuration (see Figure 5 of ref 5).

For simplicity, Devonshire[34] approximated $V(\Theta,\Phi)$ by an analytic expression which maintains the octahedral symmetry and allows for a straightforward (though lengthy[34,37]) evaluation of the corresponding librational eigenenergies:

$$V(\Theta,\Phi) \approx V_D(\Theta,\Phi) \equiv Kv(\Theta,\Phi) \quad (11)$$

(the subscript D means Devonshire) where

$$v(\Theta,\Phi) = -\frac{1}{8}(3 - 30\cos^2\Theta + 35\cos^4\Theta + 5\sin^4\Theta\cos 4\Phi) \quad (12)$$

and K is a constant which may be adjusted to reproduce the barrier of $V(\Theta,\Phi)$. Similarly, as a first approximation, it is convenient to employ the same functional form for $\tilde{V}(\Theta,\Phi)$:

$$\tilde{V}(\Theta,\Phi) \approx \tilde{V}_D(\Theta,\Phi) \equiv \tilde{V}_0 + \tilde{K}v(\Theta,\Phi) \quad (13)$$

where $\tilde{V}_0$ is an unimportant constant. The minima and maxima

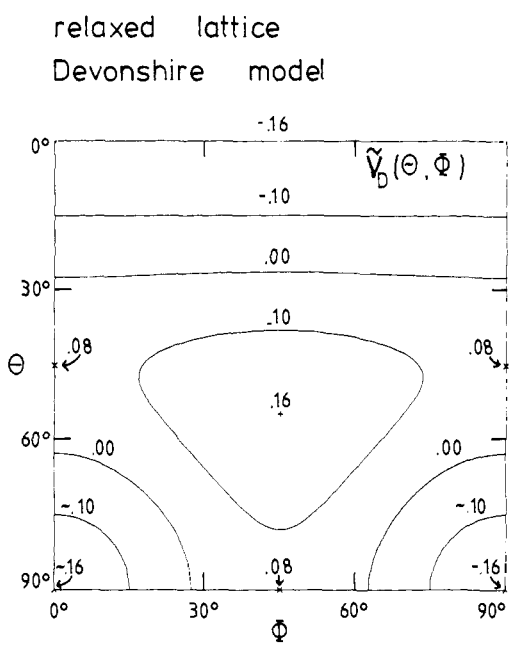

Figure 6. Devonshire approximation $\tilde{V}_D(\Theta,\Phi)$ of the relaxed potential $\tilde{V}(\Theta,\Phi)$ for CO in Ar. $\tilde{V}_D(\Theta,\Phi)$ is the interaction energy when the CO orientation is (Θ,Φ), the center of interaction is at the origin, and the Ar atoms are relaxed to their minimum-energy configuration. $\tilde{V}_D$ is fitted to $\tilde{V}$ at $(\Theta,\Phi) = (0°,0°)$ and $(54.7°,45°)$.

of $\tilde{V}_D$ are attained as

$$\tilde{V}_D(0°,0°) = \tilde{V}_0 - \tilde{K}$$
$$\tilde{V}_D(54.7°,45°) = \tilde{V}_0 + \frac{2}{3}\tilde{K} \quad (14)$$

respectively. The parameters $\tilde{V}_0$ and $\tilde{K}$ may now be adjusted to reproduce the values (10):

$$\tilde{V}_0 = 0.03 \text{ kJ mol}^{-1} = 2.7 \text{ cm}^{-1}$$
$$\tilde{K} = 0.19 \text{ kJ mol}^{-1} = 16.0 \text{ cm}^{-1} \quad (15)$$

The resulting potential $\tilde{V}_D(\Theta,\Phi)$ is shown as a contour plot in Figure 6.

We note that, in spite of the formal similarity of eq 11 and 13, there is a very important difference in their justifications. In the original Devonshire model, the impurity "sees" octahedral symmetry due to the *geometry* of the rigid lattice. In contrast, the instantaneous geometry around the impurity is a synchronously distorted octahedron, suggesting a lower than octahedral symmetry on pure geometrical grounds. However, the octahedral symmetry is restored in eq 13 since corresponding equivalent reorientations of the impurity lead to equivalent geometrical lattice distortions (be they distorted octahedrons or not!). For example, from the discussion of Figure 2 it is evident that the same value is obtained for the relaxed potential energy $\tilde{V}(\Theta,\Phi)$ when the impurity axis points to any of the six octahedral corners, i.e., along the lattice axes. A more sophisticated explanation of the restoration of the octahedral symmetry in eq 13 can be given on the grounds of modern group theory:[54] the relaxed potential (13) displays the symmetry of the system's *Hamiltonian*, which is in general higher than the point group of the instantaneous equilibrium configuration.

The advantage of the approximation (13) is that the corresponding librational eigenenergies E are already available; see ref 34 and 37. They are replotted in Figure 7, for arbitrary values of K and the rotational constant, B.

The proper value B of the rotational constant is determined using the result of section II. Since B is reciprocal to the moment of inertia, eq 9 yields

Table I. Librational Transition Frequencies of CO in Argon According to the Generalized Devonshire Model[a]

transition	Δn[b]	$\Delta\omega$/cm^{-1} [c]
$A_{1g} \rightarrow T_{1u}$	0	1.8
$T_{1u} \rightarrow E_g$	0	1.4
$E_g \rightarrow T_{1u}$	0	−1.4
$T_{1u} \rightarrow A_{1g}$	0	−1.8
$A_{1g} \rightarrow T_{1u}$	1[d]	15.2
$A_{1g} \rightarrow T_{2u}$	1	17.2
$E_g \rightarrow T_{1u}$	1	11.6
$E_g \rightarrow T_{2u}$	1	13.6
$T_{1u} \rightarrow T_{2g}$	1	9.8

[a] The model of rotating molecules in pseudorotating cages yields the Devonshire-model parameters $\tilde{B} = 1.2$ cm^{-1}, $\tilde{K} = 16.0$ cm^{-1}, i.e., $\tilde{K}/\tilde{B} = 13.3$. [b] For larger values of K/B, the lower levels A_{1g}, T_{1u}, and E_g correspond to $n = 0$, whereas the more excited levels T_{2g}, T_{1u}, and T_{2u} correspond to $n = 1$. [c] Cf. Figure 7. [d] The experimental value for $\Delta n = 1$ is a broad band centered at $\Delta\omega \approx 11.4$ cm^{-1}.[40]

$$\tilde{B} = B(I_0/I) = 1.2 \text{ cm}^{-1} \tag{16}$$

where we used the gas value, $B = 1.931\ 28$ cm^{-1}, of $^{12}C^{16}O$.[50] From eq 15 and 16

$$\tilde{K}/\tilde{B} = 13.3 \tag{17}$$

and the corresponding librational energies (in units of $\tilde{B}$) can be read directly from Figure 7.

IV. Results

In this section, we present the results obtained from an application of the theory to the special case of a CO molecule rotating in the pseudorotating cage of an Ar matrix. As is evident from Figure 7, the reorientation of CO in Ar is in the transition region between free rotation and libration.

In Table I we list the corresponding lowest frequencies of the symmetry-allowed librational transitions. They can be roughly grouped into four transitions, $\Delta n = 0$, with frequency ± 1 cm^{-1} and five transitions, $\Delta n = 1$, in the range 10–17 cm^{-1}, where Δn corresponds to the librational quantum number assignment. We note that these results are in rough accordance with the narrow $\Delta n = 0$ band and the broad $\Delta n = 1$ librational band centered at 11.4 cm^{-1}, as observed by Dubost.[39,40,43] Figure 7 also shows that the degeneracy of the $n = 1$ librational levels is much larger than the degeneracy of the $n = 0$ levels. This suggests considerable contributions to the temperature broadening of the librational bands, as observed experimentally[39,40] (for a discussion of other contributions to the line width, see ref 5 and 43). Note that the effective rotational constant, eq 16, corresponds to only $\tilde{B} = 1.6$ K; i.e., at 6 K (the lowest experimental temperature[44]) levels A_{1g}, T_{1u}, and E_g are all populated to a considerable extent, whereas the higher levels T_{2g}, T_{1u}, T_{2u}, etc., interfere as soon as $T \gtrsim 13$, 16, 19 K, etc., respectively. Furthermore, the intensities $I_{\Delta n}$ of librational Δn transitions vary roughly as[35]

$$I_{\Delta n} \approx (2\tilde{B}/\Delta\omega)^{\Delta n} \tag{18}$$

Using the value, eq 16, for $\tilde{B}$, and $\omega \approx 12$ cm^{-1}, cf. Table I, yields $I_{\Delta n} \approx 0.2^{\Delta n}$. Actually the estimate (18) has been derived in ref 35 for the librational limit where $\Delta\omega$ is larger, $\Delta\omega \gtrsim 40$ cm^{-1} (cf. Figure 7), so that the intensities should decrease even more dramatically with increasing Δn. In any case, the result (18) is again in rough agreement with the experimental result:[39,40] the $\Delta n = 1$ intensity is approximately an order of magnitude smaller than the $\Delta n = 0$ intensity, whereas the $\Delta n = 2$ librational transition is not observable within the weak phonon sidebands (which are again an order of magnitude smaller in intensity; precise values of intensities are not given in ref 39 and 40).

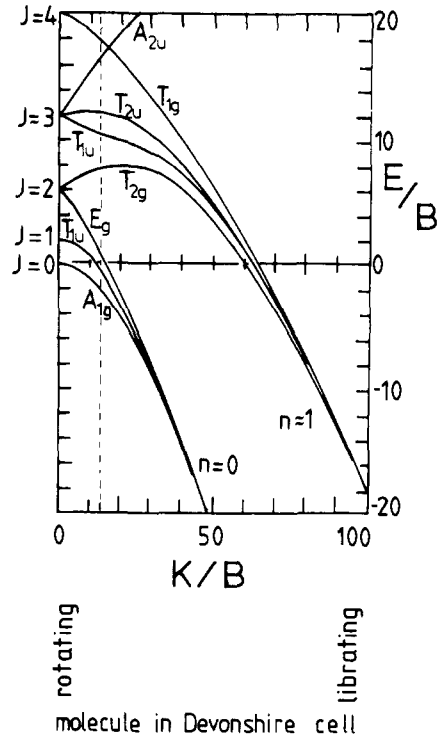

Figure 7. Librational energies E as functions of the rotational constant B and the barrier parameter K of the Devonshire cell model adapted from ref 34. The model of rotating molecules in pseudorotating cages yields $\tilde{B} \approx 1.2$ cm^{-1} and $\tilde{K} = 16.0$ cm^{-1} for CO in Ar. The corresponding librational energies are determined by the dashed line at $K/B = 13.2$, i.e., in the transition region between free rotation (quantum numbers J) and libration (quantum numbers n).

V. Discussion

It is interesting to contrast the agreement of the experimental[39,40,43] findings and the present results with the disagreement obtained without the model of the rotating molecule in the pseudorotating cage. In the latter case, $K = 0.50$ kJ mol$^{-1} = 41.6$ cm^{-1} (cf. eq 10 and 14), and the values of B are $1.931\ 28$ cm^{-1} [50] or 1.61 cm^{-1} [40] in the gas, and including the molecular center of mass rotation around the center of interaction, respectively (cf. eq 4, 9, and 16. Using the corresponding values of $K/B \approx 21$ or ≈ 26 in the Devonshire model, Figure 7 yields values of the librational frequency $\Delta\omega \approx 25$ or 23 cm^{-1}, twice as large as the present and the experimental value, ≈ 12 cm^{-1}.

Of course, the model of the rotating molecule in the pseudorotating cage does not require the approximation (13). Instead, $\tilde{V}(\Theta,\Phi)$ could be computed directly (e.g., in a force-field calculation) and used in a numerical solution of the Schrödinger equation for the librational eigenenergies and -functions:

$$(\mathcal{L}^2/2I + \tilde{V})\,\psi = E\psi \tag{19}$$

where $\mathcal{L}$ is the angular momentum operator. The numerical computation of $\tilde{V}$ and the solution of (19) may exploit the octahedral symmetry ($\tilde{V}(\Theta,\Phi)$ need be computed on only $^1/_{48}$ of the 4π sphere $[(\Theta,\Phi)]$) as well as the fact that non-nearest-neighbor atoms essentially do not participate in the lattice relaxation the minimum of $\tilde{V}(\Theta,\Phi)$ needs to be found in a configuration space of dimension not exceeding $12 \times 3 + 1 = 37$). Furthermore, since the pseudorotational cage deformation is an intermolecular effect, the minimum potential $\tilde{V}(\Theta,\Phi)$ is insensitive to three-body interactions depending on intramolecular coordinates.[5] Comparison of the topologies of the undistorted potential $\tilde{V}(\Theta,\Phi)$ (see Figures 4 and 5), with $\tilde{V}_D(\Theta,\Phi)$ (see Figure 6) suggests that the maxima of V_D are

actually saddle points of the exact V; the maximum values of V should then slightly exceed 0.16 kJ mol^{-1}, and the librational character of the spectrum would be more pronounced. Therefore, we expect that the exact solution of eq 19 should also lead to a $\Delta n = 1$ librational band centered at ≈ 12 cm^{-1}, but the $\Delta n = 0$ and 1 bands should be narrower than in Table I, in accordance with the experimental findings.

VI. Conclusions

In this paper, we have introduced the model of the rotating molecule in the pseudorotating cage. The model has been used to generalize the Devonshire cell model,[34] which implements a rigid cage for the rotating molecule. Two important effects of the nonrigidity of the lattice are incorporated. Firstly, for a given molecular orientation, the molecule–crystal interaction potential energy is minimized by lattice relaxations, thus replacing the potential for the molecule in the undistorted lattice. Secondly, the orientation-dependent lattice relaxations induce an increase of the effective moment of inertia associated with the coupled molecular and host rotation and pseudorotation. The resulting Schrödinger equation, eq 19, is nevertheless no more complicated than for the original Devonshire model, provided that similar potential approximations are employed. From eq 13 approximate librational spectra can be deduced directly from Devonshire's energy diagrams,[34] however, with "reduced" barrier and rotational constants, $\tilde{K}$ and $\tilde{B}$, according to the two effects of the pseudorotating cage.

The approximate form of the increased effective moment of inertia, eq 9, suggests an interesting isotope effect. The first contribution, i.e., the well-known rotation of the center of mass around the center of interaction, increases with the guest molecular mass. The second contribution, i.e., the pseudorotation, increases with the host molecular masses; cf. eq 4 and 8, respectively.

We should like to point out that similar increased effective moments of inertia (or corresponding rotational constants) are already known in the field of molecular internal rotations, e.g., of molecular "top"-side groups spinning with respect to the rest "frame" (see, for example, ref 51). However, there is an important difference between physical mechanisms: in internal rotations, the increased moment of inertia essentially arises from the distortions of the top which increase with increasing rotational quantum number, i.e., the corresponding effective rotational constants decrease. On the other hand, the faster the rotation of a matrix-isolated molecule, the smaller should be the cage's pseudorotational ability to follow the rotation; i.e., we predict increasing effective rotational constants with increasing rotational quantum number. A corresponding effect in molecular internal rotations would require deformations of the frame.

The model has been exemplified for the case of CO in Ar, yielding qualitative agreement with the experimental librational spectrum. In particular, the sublevels of the first librational excitation, $n = 1$, have energies $\approx 13 \pm 3$ cm^{-1}, clearly below the typical argon phonon energies $\omega_D \approx 63.9$ cm^{-1}.[52] The model assumption that the librational motion is slow in comparison with lattice vibrations is therefore justified for the case of CO in Ar. We note that, for molecules with very large rotational constants, such as the hydrazides, the frequency relations may be reversed, and one is then in the regime of complementary theories, e.g., ref 20. The present model is expected to apply in particular for heavier molecules trapped in pseudorotating cages.

Acknowledgment. I should like to express my thanks to Dr. A. Blumen, Professor G. L. Hofacker, Dr. K. Mirsky, Dr. N. Rösch, and Dr. G. Zumofen for helpful discussions, to Prof. D. J. Diestler for his exemplary work on the manuscript, and to Dr. H. Dubost and Professor S. Kimel for giving me preprints of their papers prior to publication. Generous financial support by the Deutsche Forschungsgemeinschaft and the Fonds der Chemischen Industrie is gratefully acknowledged.

References and Notes

(1) D. Maillard, A. Schriver, J. P. Perchard, C. Girardet, and D. Robert, *J. Chem. Phys.*, **67**, 3917 (1977).
(2) C. Girardet, D. Maillard, A. Schriver, and J. P. Perchard, *J. Chem. Phys.*, **70**, 1511 (1979).
(3) P. L. Kunsch, *J. Chem. Phys.*, **70**, 1343 (1979).
(4) D. P. Craig, B. R. Markey, and A. O. Griewank, *Chem. Phys. Lett.*, **62**, 223 (1979).
(5) J. Manz and K. Mirsky, *Chem. Phys.*, in press.
(6) K. O. Lee, *Can. J. Phys.*, **49**, 2018 (1971).
(7) L. E. Brus and V. E. Bondybey, *J. Chem. Phys.*, **63**, 786 (1975).
(8) V. E. Bondybey and L. E. Brus, *J. Chem. Phys.*, **63**, 794 (1975).
(9) V. E. Bondybey, *J. Chem. Phys.*, **65**, 5138 (1976).
(10) J. Goodman and L. E. Brus, *J. Chem. Phys.*, **67**, 4408 (1977).
(11) J. Goodman and L. E. Brus, *J. Chem. Phys.*, **67**, 4858 (1977).
(12) J. Goodman and L. E. Brus, *J. Chem. Phys.*, **69**, 1853 (1978).
(13) L. Abouaf-Marguin, B. Gauthier-Roy, and F. Legay, *Chem. Phys.*, **23**, 443 (1977).
(14) F. Legay in "Chemical and Biochemical Applications of Lasers", Vol. 2, C. B. Moore, Ed., Academic Press, New York, 1977, p 43.
(15) K. F. Freed and H. Metiu, *Chem. Phys. Lett.*, **48**, 262 (1977).
(16) M. Berkowitz and R. B. Gerber, *Chem. Phys. Lett.*, **49**, 260 (1977).
(17) R. B. Gerber and M. Berkowitz, *Phys. Rev. Lett.*, **39**, 1000 (1977).
(18) R. B. Gerber, M. Berkowitz, and V. Yakhot, *Mol. Phys.*, **36**, 355 (1978).
(19) R. B. Gerber and M. Berkowitz, *Chem. Phys. Lett.*, **56**, 105 (1978).
(20) M. Berkowitz and R. B. Gerber, *Chem. Phys.*, **37**, 369 (1979).
(21) D. Knittel and S. H. Lin, *Mol. Phys.*, **36**, 893 (1978).
(22) D. J. Diestler, E.-W. Knapp, and H. D. Ladouceur, *J. Chem. Phys.*, **68**, 4056 (1978).
(23) G. Zumofen and K. Dressler, *J. Chem. Phys.*, **64**, 5198 (1976).
(24) G. Zumofen, *J. Chem. Phys.*, **68**, 3747 (1978).
(25) G. Zumofen, *J. Chem. Phys.*, **69**, 4264 (1978).
(26) H. Friedmann and S. Kimel, *J. Chem. Phys.*, **43**, 3925 (1965).
(27) H. Friedmann and S. Kimel, *J. Chem. Phys.*, **47**, 3589 (1967).
(28) P. D. Mannheim and H. Friedmann, *Phys. Status Solidi*, **39**, 409 (1970).
(29) L. F. Keyser and G. W. Robinson, *J. Chem. Phys.*, **44**, 3225 (1966).
(30) E. Blaisten-Barojas and M. Allavena, *J. Phys. C*, **9**, 3121 (1976).
(31) J. Vitko, Jr., and C. F. Coll, III, *J. Chem. Phys.*, **69**, 2590 (1978).
(32) P. L. Kunsch and K. Dressler, *J. Chem. Phys.*, **68**, 2550 (1978).
(33) L. Pauling, *Phys. Rev.*, **36**, 430 (1930).
(34) A. F. Devonshire, *Proc. R. Soc. London, Ser. A*, **153**, 601 (1936).
(35) R. M. Hexter and D. A. Dows, *J. Chem. Phys.*, **25**, 504 (1956).
(36) W. H. Flygare, *J. Chem. Phys.*, **39**, 2263 (1963).
(37) P. Sauer, *Z. Phys.*, **194**, 360 (1966).
(38) H. E. Hallam, Ed., "Vibrational Spectroscopy of Trapped Species", Wiley, New York, 1973.
(39) H. Dubost, Thèse, Université Paris XI, 1975.
(40) H. Dubost, *Chem. Phys.*, **12**, 139 (1976).
(41) H. Dubost and R. Charneau, *Chem. Phys.*, **12**, 407 (1976).
(42) H. Dubost and R. Charneau, *Chem. Phys.*, **41**, 329 (1979).
(43) H. Dubost, A. Lecuyer, and R. Charneau, *Chem. Phys. Lett.*, **66**, 191 (1979).
(44) J. Manz, *Chem. Phys.*, **24**, 51 (1977).
(45) J. Manz, *Chem. Phys. Lett.*, **51**, 477 (1977).
(46) A. Blumen, J. Manz, and V. Yakhot, *Chem. Phys.*, **26**, 287 (1977).
(47) A. Blumen, S. H. Lin, and J. Manz, *J. Chem. Phys.*, **69**, 881 (1978).
(48) R. D. Levine and J. Manz, *Chem. Phys.*, **33**, 151 (1978).
(49) J. Manz, to be published.
(50) J. F. Ogilvie, *J. Mol. Spectrosc.*, **69**, 169 (1978).
(51) M. Ribeaud, A. Bauder, and Hs. H. Günthard, *Mol. Phys.*, **23**, 235 (1972).
(52) C. Kittel, "Introduction to Solid State Physics," 4th ed., Wiley, New York, 1971.
(53) H. Friedmann and S. Kimel, *J. Chem. Phys.*, in press.
(54) P. R. Bunker, "Molecular Symmetry and Spectroscopy", Academic Press, New York, 1979.